

Direct ethanol fuel cell (DEFC): Electrical performances and reaction products distribution under operating conditions with different platinum-based anodes

S. Rousseau, C. Coutanceau*, C. Lamy, J.-M. Léger

Laboratoire de Catalyse en Chimie Organique, "Equipe Electrocatalyse" UMR-CNRS 6503, Université de Poitiers, 40 Avenue du Recteur Pineau, 86022 Poitiers Cedex, France

Received 17 January 2005; accepted 23 August 2005

Available online 19 October 2005

Abstract

Ethanol electro-oxidation at different Pt-based electrodes was investigated in a single direct ethanol fuel cell (DEFC) in terms of reaction product distribution depending on the anode catalyst. In DEFC experiments, only three reaction products were detected using HPLC: acetaldehyde (AAL), acetic acid (AA) and CO₂. The addition of tin to platinum increases the activity of the catalyst by several order of magnitude and the electrical performance of the DEFC are greatly enhanced from a few mW cm⁻² to 30 mW cm⁻² at 80 °C, with Pt/C and Pt–Sn/C catalysts, respectively. Moreover, at Pt–Sn/C and Pt–Sn–Ru/C the formation of CO₂ and AAL is lowered whereas the formation of AA is increased in comparison to what happens at a Pt/C catalyst. The addition of Ru to Pt–Sn only leads to enhance the electrical performance of the DEFC, i.e. the activity of the catalyst, but does not modify the product distribution. Very good stability in the open circuit voltage of the DEFC (close to 0.75 V) was observed over a period of 2 weeks at 90 °C, the cell undergoing start-run-stop cycles each day. Good stability under operating conditions at a given current density was also observed over 6 h.

© 2005 Elsevier B.V. All rights reserved.

Keywords: Direct ethanol fuel cell; Long term stability; Products distribution; Platinum; Ruthenium; Tin

1. Introduction

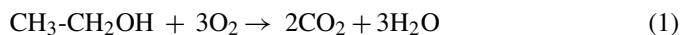
The study of the electro-oxidation of alcohols has a direct application, which is their use as an alternative fuel in fuel cells. While pure hydrogen or hydrogen-rich gases allow to obtain higher electric efficiency than alcohols in a proton exchange membrane fuel cell (PEMFC), their production, storage and distribution are still brakes for a large scale development [1–3]. In this context, the use of hydrogen carrier like alcohols in a direct alcohol fuel cell (DAFC) appears advantageous for two main reasons: they are liquid (which simplifies the problems of storage and distribution) and their theoretical mass energy density is rather high (6.1 and 8.0 kWh kg⁻¹ for methanol and ethanol, respectively [4]). The most studied alcohols are methanol [5–8], which is the simplest one, and ethanol [9–11].

Methanol is known to achieve a power density at 90 °C between 200 and 300 mW cm⁻² in a direct methanol fuel cell (DMFC) [12–14], which is higher than that obtained with ethanol (close to 50 mW cm⁻²) [15,16]. However, the electro-oxidation of methanol at platinum-based electrodes was extensively studied for the last 20–30 years, conversely to the electro-oxidation of ethanol, and it can be thought that improvement in the electrocatalysis of ethanol oxidation can be made. Moreover, methanol is a toxic compound and its use in large scale can cause some environmental and safety problems. On the other hand, ethanol can be obtained from biomass. In this case, the use of bioethanol as a fuel will not change the natural balance of carbon dioxide in the atmosphere in contrast to the use of fossil fuels [1]. These reasons motivate investigations on ethanol electro-oxidation in order to improve the electrical performances when using it in a direct ethanol fuel cell (DEFC), and to open the possibility of replacing methanol in a DAFC.

But, ethanol contains two bonded carbon atoms. Therefore, to achieve the maximum theoretical electric energy, it is necessary to break the C–C bond and to form CO₂ as reaction product,

* Corresponding author. Tel.: +33 5 49 45 48 95; fax: +33 5 49 45 35 80.
E-mail address: christophe.coutanceau@univ-poitiers.fr (C. Coutanceau).

according to the following equation:



In that case, the oxidation of ethanol involves the transfer of 12 electrons. But, it is known that ethanol oxidation at platinum electrodes leads to the formation of other reaction products than CO_2 , like acetic acid (AA), acetaldehyde (AAL) [17–19], . . . , etc. To form these reaction products, the transfer of four and two electrons, respectively, is required, which obviously leads to decrease the total efficiency of a DEFC. Therefore, it is very important to identify the reaction intermediates and products in order to formulate the best catalyst composition, structure, . . . , etc. It is also important to determine the long term stability of anodes containing metals like platinum and tin. Indeed, the first metal is known to be easily poisoned by adsorbed species coming from the dissociative adsorption of ethanol [20,21] and then to deactivate rapidly, whereas the second metal can form irreversible oxides (SnO_2), which are inactive for the reaction [22], or can dissolve in acid medium at mean potentials as it is the case for molybdenum [23]. The fuel cell tests must give some information about synergetic effects between platinum and tin towards ethanol electro-oxidation.

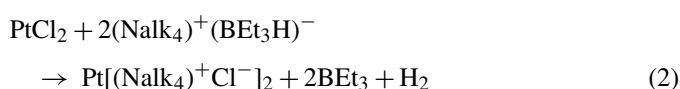
The main goal of this paper is to investigate the electro-oxidation of ethanol at platinum-based catalysts (Pt/C, PtSn/C and PtRuSn/C) under DEFC operating conditions. For that, the reaction product distribution, the electrical stability and performance of the DEFC were determined under fuel cell operation at several working voltages (current densities) of the cell.

2. Experimental

2.1. Preparation of the carbon supported Pt-based electrocatalysts

The preparation method of the Pt/C, PtSn/C and PtSnRu/C catalysts is based on the synthesis of colloidal precursors using the procedure described by Bönemann et al. [24], slightly modified.

The preparation method was described elsewhere [25,26]. Briefly, the synthesis method is as follows. The first step consisted in the synthesis of the reducing agent by mixing a stoichiometric amount of tetra(alkyl)ammonium bromide $(\text{Nalk}_4)^+\text{Br}^-$ and potassium triethylhydroborate $\text{K}^+(\text{BEt}_3\text{H})^-$ in tetrahydrofuran (THF) as solvent. After elimination of the precipitated KBr, a solution of tetra(alkyl)ammonium triethylhydroborate $(\text{Nalk}_4)^+(\text{BEt}_3\text{H})^-$ was obtained which reduced the platinum, ruthenium or tin salts according to the following reaction, written in the case of platinum:



In this way, the platinum nanoparticles are stabilized by $(\text{Nalk}_4)^+\text{Cl}^-$, which acts as a surfactant protecting the metal particles by its long alkyl chain.

The colloid particles were adsorbed on VULCAN XC 72, previously treated for 4 h at 400°C under nitrogen to clean it, in

order to obtain a catalyst loading of 60 wt.% based on the metal content. Before using them as electrocatalysts, the organic surfactant shell of the supported colloid catalysts must be removed by a thermal treatment under air atmosphere at 300°C .

2.2. Physical and electrochemical characterizations

Characterizations of the catalyst particles so obtained were carried out by different physical techniques: transmission electron microscopy (TEM) for a morphological observation of their surface with determination of the particle size and including an estimation of the particle composition by energy dispersive analysis of X-rays (EDX), and X-ray diffraction (XRD) to determine the catalyst structure and evaluate the particle size. Typical results of such characterizations are given elsewhere for a Pt–Sn/C catalyst [19]. For example, it was shown that the mean particle size is 2.7 ± 1.2 nm.

2.3. Preparation of the electrodes and membrane electrode assemblies (MEAs)

Electrodes were prepared from an ink made with the supported catalyst and a Nafion[®] solution according to a method described elsewhere [15,25]. It consists in painting a catalytic ink (dispersion in absolute ethanol-Sigma of the catalytic powder and Nafion[®] 5 wt.% in aliphatic alcohol-Aldrich) at the surface of a diffusion layer (C + PTFE 20 wt.%) and to dry it. The metal loading of the anode was 3 mg cm^{-2} , with a 60% Pt-based/C catalyst and 0.8 mg cm^{-2} of Nafion[®].

The MEAs were prepared by hot pressing at 130°C for 90 s under a pressure of 35 kg cm^{-2} , a pre-treated Nafion[®] 117 membrane with an E-TEK cathode (2.0 mg cm^{-2} Pt loading, 40% metal/C, 40% PTFE, 0.8 mg cm^{-2} Nafion[®]) and with the home-made anodes.

2.4. Direct ethanol fuel cell tests

Fuel cell tests in a single cell with a 25 cm^2 geometric surface area were carried out with a Globe Tech test bench. The E versus j and P versus j curves were recorded using a high power potentiostat (Wenking model HP 88) interfaced with a PC to apply constant current sequences and to store the data, and a variable resistance in order to fix the current applied to the cell.

2.5. HPLC analyses

A high performance liquid chromatograph (Dionex CHROMELEON) fitted with an isocratic pump, an auto-sampler, an UV detector and a refractometer detector was used to analyse quantitatively the reaction products at the outlet of the anode side of the DEFC.

Fig. 1 presents the set-up for trapping the outlet products. In the first flask, ethanol, acetic acid and acetaldehyde in solution can be directly analysed by HPLC. In the second flask, the volatile acetaldehyde transported by the nitrogen flow from the first flask reacts with an excess of a 0.45 wt.% 2,4-

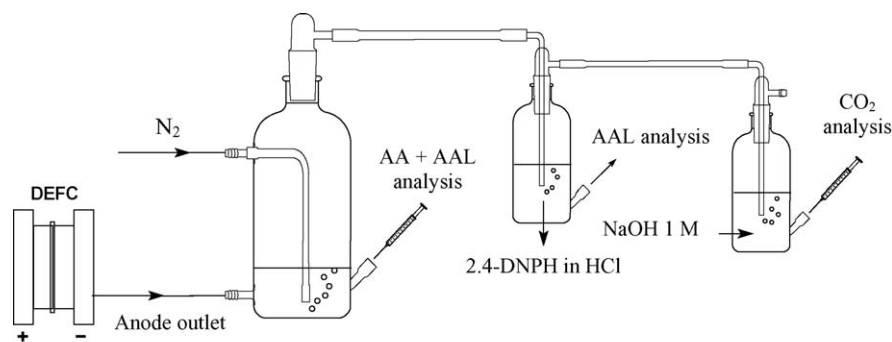
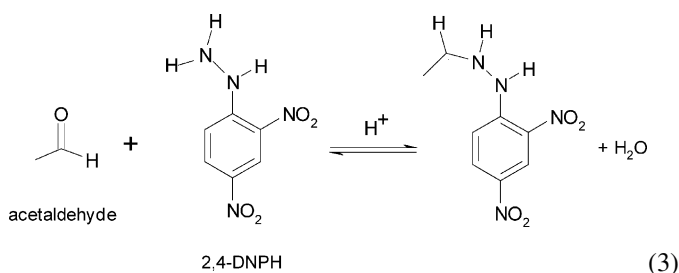


Fig. 1. Experimental set-up to trap the reaction products at the outlet of the DEFC before HPLC analysis.

dinitrophenylhydrazine (DNPH) in a 2.0 M HCl solution according to the following equation:



The orange precipitate is then solubilized in ethyl acetate and analysed by HPLC.

In the third flask, the formed CO_2 is transported by the nitrogen flow and reacts with a 1.0 M sodium hydroxide solution to form carbonate CO_3^{2-} anions. The CO_3^{2-} ions are detected in HPLC because of the formation of a negative peak.

Two different columns were used according to the products to be analysed. For AAL, AA and CO_3^{2-} analysis an HPX-87H column was used with an eluent (0.01 M H_2SO_4 solution) flow of 0.6 mL min^{-1} . For hydrazone derivative, a C18-NH₂ column was used with an eluent ($\text{CH}_3\text{CN}/\text{H}_2\text{O}$ 60:40) flow of 0.6 mL min^{-1} .

AA and AAL can be detected by the UV detector at a wavelength of 240 nm as well as by the refractometer detector, whereas CO_3^{2-} was only detected using the refractometer.

3. Results and discussion

3.1. Electrical performance and stability of the DEFC

Fuel cells test were carried out at different cell voltages with Pt/C, Pt–Sn/C, Pt–Sn–Ru/C catalysts in order to determine the distribution of reaction products under operating conditions: 80°C , 3 bar O_2 (flow rate 300 mL min^{-1}) and $[\text{EtOH}] = 2 \text{ M}$, $P_{\text{EtOH}} = 1 \text{ bar}$ (flow rate 10 mL min^{-1}). Fig. 2 shows the $E(j)$ and $P(j)$ curves obtained with a single DEFC of 25 cm^2 . First, it can be seen that platinum alone as anode catalyst leads to poor electrical performance, the open circuit voltage (OCV) being lower than 0.5 V and the maximum current density reaching only 15 mA cm^{-2} , leading to a maximum power density lower than 5 mW cm^{-2} . The addition of Sn to platinum in the anode, even in low amount (in our case 10 at.%), leads to greatly enhance the

electrical performance of the DEFC by increasing the OCV up to 0.7 V and current densities up to 120 mA cm^{-2} giving a maximum power density close to 30 mW cm^{-2} , which means electrical performances ten times higher than those obtained with Pt/C. Addition of 4 at.% of Ru to Pt–Sn allows again to enhance the electrical performance of the DEFC up to 50 mW cm^{-2} for a current density of 180 mA cm^{-2} , the OCV being close to 0.75 V. These experiments show clearly the benefit obtained by alloying Pt with Sn and Ru. The increase of the OCV indicates that the bi- and tri-metallic catalysts are less poisoned by adsorbed species from ethanol than the Pt/C catalyst. The increase of the electrical performance indicates that the bi- and tri-metallic catalysts are more active for ethanol electro-oxidation than the Pt/C catalyst, which is in agreement with other previous published results [16,27,28].

Before to determine the distribution of reaction products under DEFC operating conditions, the stability of the cell voltage was examined over 4 h. The cell voltage appears to be very stable when, for instance, a current of 32 mA cm^{-2} was applied, remaining between 0.45 and 0.5 V in the case of a DEFC mounted with a Pt–Sn (9:1)/C anode (Fig. 3). The same behaviour was observed with a Pt–Sn–Ru (86:10:4)/C, the cell voltage remaining close to 0.6 V under the same working conditions.

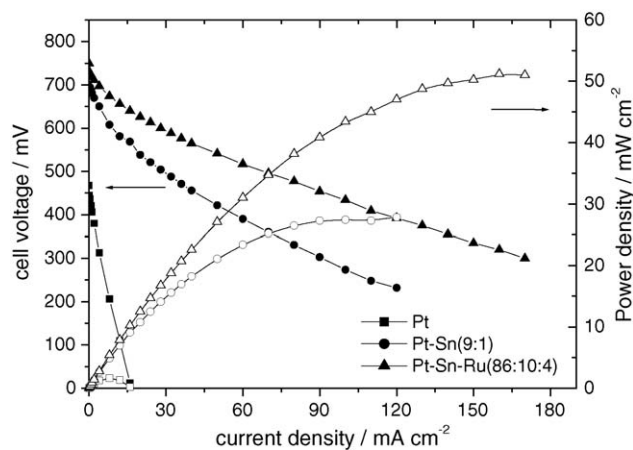


Fig. 2. Fuel cell characteristics of a 25 cm^2 DEFC recorded at 80°C . Influence of the composition of the Pt-based bimetallic anode (3 mg cm^{-2} Pt loading, 60 wt.% catalyst on carbon). $P_{\text{O}_2} = 3 \text{ bar}$; $P_{\text{EtOH}} = 1 \text{ bar}$; $[\text{EtOH}] = 2 \text{ M}$; Nafion® 117 membrane.

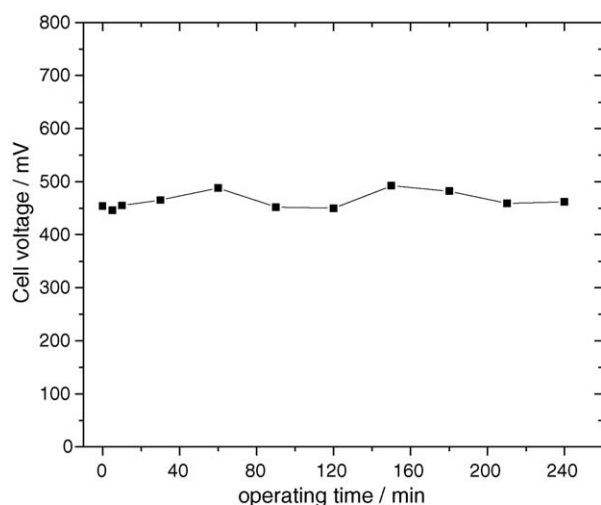


Fig. 3. Cell voltage of the DEFC with a Pt–Sn (9:1)/XC72 anode (3 mg cm^{-2} Pt loading, 60 wt.% catalyst on carbon) vs. time with $j = 32 \text{ mA cm}^{-2}$, $T = 80^\circ \text{C}$; $P_{\text{O}_2} = 3 \text{ bar}$; $P_{\text{EtOH}} = 1 \text{ bar}$; $[\text{EtOH}] = 2 \text{ M}$; Nafion[®] 117 membrane.

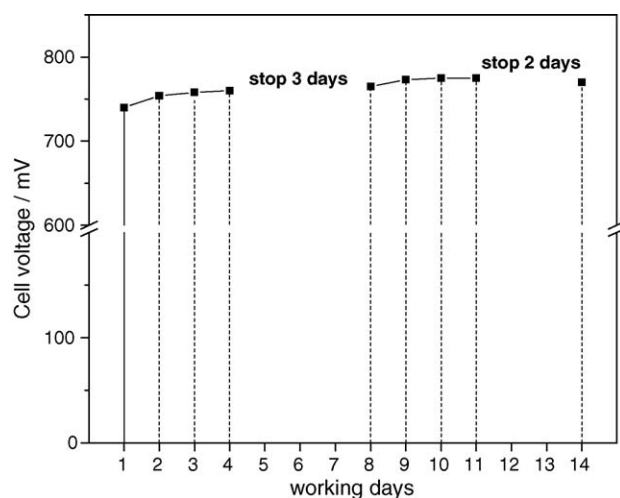


Fig. 4. Open circuit voltage recorded at 80°C for 14 days before start-stop-run cycles of a DEFC with a Pt–Sn (9:1)/XC72 anode (3 mg cm^{-2} Pt loading, 60 wt.% catalyst on carbon).

Moreover, fuel cell experiments were carried out at a temperature of 80°C over 14 days. Fig. 4 reports the value of the open circuit voltage of a DEFC, fitted with a PtSn (9:1)/C anode, as a function of time. Each day, the open circuit voltage of the cell was measured, and then start-run-stop cycles were carried out in order to obtain and compare the $E(j)$ and $P(j)$ curves and to

determine the distribution of reaction products. It appears that, if the cell is working under a current density range lower than 100 mA cm^{-2} , i.e. if the cell voltage does not reach values lower than 0.3 V – corresponding to an anode potential close to 0.5 V versus RHE, assuming a cathode potential close to 0.8 V versus RHE – the DEFC displays a very good long term stability. When the working voltage is lower than 0.3 V , the DEFC performances decreased drastically and become lower than those obtained with platinum alone. To explain this fact, it is proposed that at these low cell voltages, i.e. high anode potentials, irreversible tin oxides are formed, which are non catalytic and less conductive.

3.2. Product distribution in DEFC experiments as a function of the cell voltage

In order to determine the reaction products, the current density was kept constant and the voltage of the cell was simultaneously measured as a function of time. The ethanol flow rate was chosen close to 2 mL min^{-1} in order to perform the experiments for at least 4 h.

Because the electrodes are homemade, fluctuations in the amount of catalyst deposited on the electrode can occur. Then, in order to make comparison in the distribution of reaction products at different current densities (i.e. at different cell voltages), or to compare different catalysts (Pt/C, Pt–Sn/C and Pt–Ru–Sn/C) in term of selectivity, it is better to express the selectivity as a non-dimensional number like the ratio between the number of moles of a formed species to the total number of moles of formed products, which corresponds rather to the chemical yield for each reaction product.

Table 1 reports the results obtained at different current densities (i.e. at different cell voltages) using a PtSn (9:1)/C catalyst. With a DEFC mounted with a Pt–Sn (9:1)/C anode, the determination by HPLC of the amount of AA, AAL and CO_2 formed at 32 mA cm^{-2} gives the following results: $[\text{AA}] = 50 \text{ mmol L}^{-1}$, $[\text{AAL}] = 10 \text{ mmol L}^{-1}$, $[\text{CO}_2] = 5 \text{ mmol L}^{-1}$. 490 mL of solution were recovered in the cell outlet. No other products were detected by chromatographic analyses. To form these products the necessary quantity of electricity can be calculated as follows:

$$q = I \times t \quad (4)$$

where q is the charge in Coulomb, I , the current intensity in ampere and t is the time in second.

Table 1

Electrical characteristics of a 25 cm^2 DEFC fitted with a Pt–Sn (9:1)/XC72 anode (3 mg cm^{-2} Pt loading, 60 wt.% catalyst on carbon) used for determination of the distribution of the reaction products after 4 h operating time and evaluation of the cross-over rate of ethanol at different current densities

j (mA cm^{-2})	E_{cell} (V)	Calculated n_e	Concentration (mmol L^{-1})				Anode outlet volume (L)	Experimental n_e	Chemical Yield (%)			Xover rate J_{norm} ($\text{mol s}^{-1} \text{ cm}^{-2}$)
			CO_2	AA	AAL	EtOH			CO_2	AA	AAL	
24	0.51–0.55	0.09	4.4	41.3	9.5	1790	0.4	0.09	8.0	74.8	17.2	0.87×10^{-7}
32	0.45–0.49	0.12	5.0	50.0	10.0	1770	0.49	0.12	7.7	76.9	15.4	1.14×10^{-7}
40	0.40–0.43	0.15	3.0	55.0	11.0	1760	0.5	0.13	4.4	79.7	15.9	1.20×10^{-7}

$T = 80^\circ \text{C}$; $P_{\text{O}_2} = 3 \text{ bar}$; $P_{\text{EtOH}} = 1 \text{ bar}$; $[\text{EtOH}] = 2 \text{ M}$; Nafion[®] 117 membrane.

Then,

$$q = 0.032 \times 25 \times 4 \times 3600 = 11520 \text{ C} \quad (5)$$

which can be expressed in moles of exchanged electron n_e :

$$n_e = \frac{11520}{96500} = 0.119 \approx 0.12 \text{ mol} \quad (6)$$

It is now possible to determine, from the estimation of the amount of each reaction products formed in the DEFC, the number of mole of electron needed to form them. First, the number of mole of each product has to be calculated:

$$n_{\text{AAL}} = 10 \times 10^{-3} \times 0.49 = 4.9 \times 10^{-3} \text{ mol} \quad (7)$$

$$n_{\text{AA}} = 50 \times 10^{-3} \times 0.49 = 2.45 \times 10^{-2} \text{ mol} \quad (8)$$

$$n_{\text{CO}_2} = 5 \times 10^{-3} \times 0.49 = 2.45 \times 10^{-3} \text{ mol} \quad (9)$$

Knowing that the formation of 1 mol of AAL, AA and CO_2 needs the transfer of two, four and six electrons, respectively, the number of moles of exchanged electrons can be calculated for each products as well as the total number of mole of exchanged electron:

$$n_e(\text{AAL}) = 4.9 \times 10^{-3} \times 2 = 9.8 \times 10^{-3} \quad (10)$$

$$n_e(\text{AA}) = 2.45 \times 10^{-2} \times 4 = 9.8 \times 10^{-2} \quad (11)$$

$$n_e(\text{CO}_2) = 2.45 \times 10^{-3} \times 6 = 1.47 \times 10^{-2} \quad (12)$$

Then, the total number of moles of electron exchanged to form the three identified products is:

$$\begin{aligned} n_e &= 9.8 \times 10^{-3} + 9.8 \times 10^{-2} + 1.47 \times 10^{-2} \\ &= 0.122 \approx 0.12 \text{ mol} \end{aligned} \quad (13)$$

The good reliability between the number of transferred electrons calculated using the current intensity and using the amount of detected products seems to indicate that no other products are formed during ethanol electro-oxidation at a Pt–Sn catalyst under DEFC operating conditions. However, it is possible that other products can be formed and not detected, notably of ethyl acetate. This latter product can be formed via the reaction between acetic acid and ethanol to form the corresponding ester. For example, at high current density, the experimental number of exchanged electrons is lower than the calculated one. Under these conditions, the concentration of AA is higher and the formation of ester is likely made easier, which lowers the experimental number of exchanged electrons.

Looking at Table 1, one can see that the main reaction product independently of the current density or anode potential is acetic acid with a yield close to 75–80%, followed by acetaldehyde with a yield between 15 and 17% and from 8 to 4% for CO_2 . It seems that, at low current densities (high cell voltages), the formation of CO_2 is favoured (twice higher) compared to that obtained at higher current densities, i.e. lower cell voltages. In a previous paper [19], we proposed on the basis of in situ IR reflectance spectroscopy measurements, that when Pt–Sn/C is used as a catalyst for ethanol electro-oxidation, the formation

of CO_2 seems to be, at least partially, disconnected from the coverage in adsorbed CO species. The amount of carbon dioxide formed with anode potentials close to 0.4 V versus RHE should be related not only to the adsorbed CO removal, but also to the further oxidation of acetaldehyde. It can then be proposed here that, assuming a cathode potential close to 1.0–0.9 V versus RHE, at a cell voltage of 0.6–0.5 V, the oxidation into CO_2 of adsorbed CO species, coming from the dissociative adsorption of EtOH and the breaking of the C–C bond, takes place at the same time as the oxidation of acetaldehyde, producing a relative high amount of CO_2 , whereas at lower cell voltage (higher current densities), no adsorbed CO species are formed from ethanol, only from acetaldehyde, which lowers the production of CO_2 . Considering the two other main products, the increase of the current density does not lead to a noticeable variation in the yield of AAL, but leads to a small yield increase of AA from 77 to 80%.

The obtained results lead to the possibility to evaluate the cross-over of ethanol during the experiments if assuming that all reaction products were detected and quantified, which is a reasonable assumption according to the good reliability between the calculated and experimental values of the number of exchanged electrons per ethanol molecule. The amount $[\text{EtOH}]_{\text{Xover}}$ of ethanol which crossed the membrane can be calculated as follows:

$$\begin{aligned} [\text{EtOH}]_{\text{Xover}} &= [\text{EtOH}]_{\text{init}} - \left([\text{EtOH}]_{\text{outlet}} + [\text{AAL}] + [\text{AA}] + \frac{1}{2}[\text{CO}_2] \right) \end{aligned} \quad (14)$$

where, $[\text{EtOH}]_{\text{init}}$ is the initial ethanol concentration (2 M) and $[\text{EtOH}]_{\text{outlet}}$ is the ethanol concentration in the anode outlet. The coefficient $\frac{1}{2}$ expresses the fact that two CO_2 molecules are formed by the complete electro-oxidation of one ethanol molecule (see Eq. (1)). For example, at 32 mA cm^{-2} , Eq. (14) gives a value of $167.5 \text{ mmol L}^{-1}$ of ethanol crossing the membrane for 4 h, which leads to a cross-over of:

$$\frac{d[\text{EtOH}]_{\text{Xover}}}{dt} = \frac{167.5 \times 10^{-3}}{4 \times 3600} = 1.163 \times 10^{-5} \text{ mol L}^{-1} \text{ s}^{-1} \quad (15)$$

corresponding to a cross-over rate J :

$$\begin{aligned} J &= \frac{1}{S} \frac{dN_{\text{EtOH}_{\text{Xover}}}}{dt} = \frac{1.163 \times 10^{-5}}{25} \times 0.49 \\ &= 2.28 \times 10^{-7} \text{ mol cm}^{-2} \text{ s}^{-1} \end{aligned} \quad (16)$$

It is worth to compare with the intrinsic permeability of a Nafion® 117 membrane, as determined at 20 °C in a classical two compartment cell, one containing a 1.0 M EtOH solution, the other containing only water, separated by a membrane of 3.14 cm^2 (Fig. 5). For that purpose, it is necessary to normalize the value of the cross-over under DEFC operating conditions to an EtOH concentration of 1.0 M. This gives a cross-over rate $J_{\text{norm}} = 1.14 \times 10^{-7} \text{ mol cm}^{-2} \text{ s}^{-1}$.

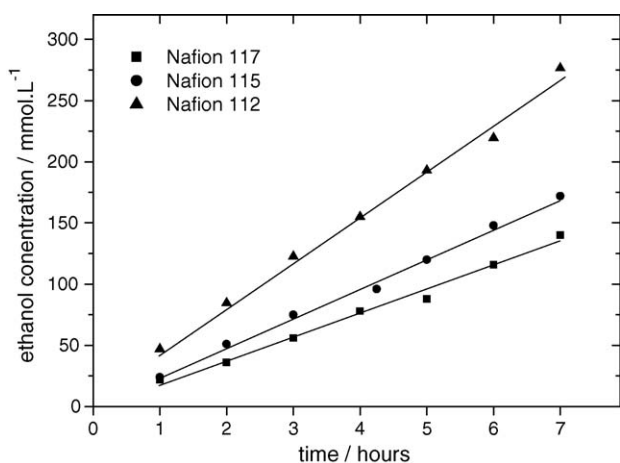


Fig. 5. Permeability to ethanol of different Nafion[®] membranes measured at 20 °C from a 1.0 M EtOH solution: (■) Nafion[®] 117; (●) Nafion[®] 115; (▲) Nafion[®] 112.

On the other hand, the intrinsic permeability of the Nafion[®] 117 membrane was found to be close to $1.72 \times 10^{-6} \text{ mol L}^{-1} \text{ s}^{-1} \text{ cm}^{-2}$ corresponding to a cross-over rate of $6.8 \times 10^{-8} \text{ mol cm}^{-2} \text{ s}^{-1}$ under our experimental conditions (cell compartments of 40 mL). For Nafion[®] 115 and 112 membranes, the evaluated cross-over rates, under the same conditions as in Fig. 5, are 8.66×10^{-8} and $13 \times 10^{-8} \text{ mol cm}^{-2} \text{ s}^{-1}$, respectively. These values are a little higher but in agreement to those given in recent papers published by Song et al. [29,30], in which they determined the cross-over of ethanol through a Nafion[®] 115 membrane. At 30 °C, they found a cross-over rate of ethanol close to $2 \times 10^{-8} \text{ mol cm}^{-2} \text{ s}^{-1}$ but with an ethanol solution flow rate of 1.0 mL min^{-1} and a nitrogen pressure of 2 bar applied in the other side of the membrane. Anyway, these results are in the same order of magnitude, which confirms the reliability of our results.

Looking at the results given in Table 1, it seems that whatever the cell voltage is, the cross-over rate at 80 °C is higher than the intrinsic permeability of the Nafion[®] 117 membrane at room temperature. This was rather expected, because one could assume that increasing the temperature would lead to increase the cross-over. But, the increase of the cross-over rate is not so important, being less than two times higher under DEFC operations, and it can be proposed as an explanation, that before reaching the membrane, ethanol has to cross the electrode structure and can react at the catalytic sites. As a consequence, the ethanol concentration in the electrode bulk should decrease from the diffusion layer/catalytic layer interface to the catalytic layer/membrane interface, and then the ethanol cross-over rate

should be lowered. It can also be shown that the cross-over of ethanol increases with increasing the current density, which can be explained by the increase of protons transportation through the membrane, which leads to increase ethanol transportation too, but the values are very close each other and no conclusion could be drawn except for the order of magnitude of this effect.

3.3. Reaction product distribution in DEFC experiments for different anode catalysts

The experiments were carried out using Pt/C, PtSn/C and Pt–Sn–Ru/C catalysts, and in each case no other reaction products than AA, AAL and CO₂ could be detected. It is generally admitted that a convenient alcohol fuel cell working voltage must be in the range of 0.4–0.6 V. For this reason, a current density of 32 mA cm^{-2} was chosen to perform the experiments for the PtSn and PtRuSn catalysts, which corresponds to a total current intensity of 800 mA, and of 8 mA cm^{-2} for the Pt/C catalyst (200 mA total intensity). Comparison between the three catalysts in term of selectivity is difficult to perform for different reasons. As it can be seen in Fig. 2, the $E(j)$ polarisation curves obtained with a DEFC mounted with a Pt/C anode does not achieve cell voltages high enough to be compared with the other catalysts. The results are recorded at cell voltages close to 0.3 V for the Pt/C anode and close to 0.45–0.55 V for the Pt–Sn/C and Pt–Sn–Ru/C anodes.

From the results given in Table 2, it appears that the addition of tin to platinum greatly favours the formation of AA comparatively to AAL. This can be explained by the bifunctional mechanism [31] where ethanol is adsorbed dissociatively at platinum sites, either via an O-adsorption or a C-adsorption process [18,32,33] to form AAL species according to the following reaction equation:



or,



or,



As soon as acetaldehyde (AAL) is formed, it can adsorb on platinum sites leading to a Pt-CH₃-CO species:



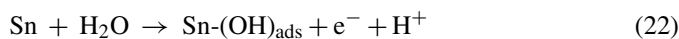
then, because Sn is known to activate water at lower potentials than platinum, some OH species can be formed at low potentials

Table 2

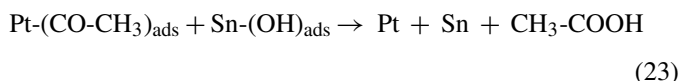
Chemical yields in AA, AAL and CO₂ for Pt/C, Pt–Sn (9:1)/C and Pt–Sn–Ru (86:10:4)/C catalysts during ethanol electro-oxidation under DEFC operating conditions at 80 °C for 4 h

	AA/products (%)	AAL/products (%)	CO ₂ /products (%)
Pt/C XC72 60 wt. %.	32.5	47.5	20.0
Pt–Sn (9:1)/C XC72 60 wt. %.	76.9	15.4	7.7
Pt–Sn–Ru (86:10:4)/C XC72 60 wt. %.	75.0	15.2	9.8

on Sn sites according to reaction:



and adsorbed acetaldehyde species can react with adsorbed OH species to produce acetic acid according to:



On the other hand, the yield in CO_2 is twice higher with a Pt/C catalyst than with a Pt–Sn/C catalyst. This can be explained by the need to have several adjacent platinum sites to adsorb dissociatively the ethanol molecule and to break the C–C bond. As soon as some tin atoms are introduced between platinum atoms, this latter reaction is disadvantaged.

At last, the addition of ruthenium to Pt–Sn/C catalysts does not change the distribution of reaction products. Its only effect is to enhance the activity towards ethanol oxidation. It was showed by Waszczuk et al. [34] that, in the case of methanol oxidation, the presence of ruthenium in a Pt-based catalyst not only allows the bifunctional mechanism to occur at lower potentials, but also involves a “ligand effect”. This effect, which is explained by a change in the electronic distribution around the platinum sites, leads to increase the rate of methanol adsorption at platinum, and then the turnover of reactant molecules on the catalytic site. As a result, the activity for methanol oxidation is enhanced.

4. Conclusion

The experiments under DEFC operating conditions led to identify the reaction products of ethanol electro-oxidation and their distribution as a function of the cell voltage and the nature of the catalyst. Only three reaction products were detected using HPLC analysis: acetaldehyde, acetic acid and CO_2 . It was shown that the addition of tin to platinum not only increases the activity of the catalyst towards the oxidation of ethanol and therefore the electrical performance of the DEFC, but also changes the product distribution: the formation of CO_2 and AAL is lowered whereas the formation of AA is increased. This was explained by the ability of tin to activate water dissociation at potentials lower than on platinum, leading to the formation of OH species necessary to complete the oxidation of ethanol via AAL adsorbed species according to the bifunctional mechanism. The addition of Ru to Pt–Sn catalyst does not involve a change in the product distribution but it enhances the electrical performance of the DEFC. The DEFC showed good electrical stability over 14 days with start-run-stop cycles, as well as during experiment where a current density was applied for 4 h.

Acknowledgement

This work was done partially under the framework of a project (convention No. 01 01 009 ADEME/AGRICE) of the French Fuel Cell Network (PACo).

References

- [1] J.W. Gosselink, *Int. J. Hydrogen Energy* 27 (2002) 1125.
- [2] N. Takeichi, H. Senoh, T. Yokota, H. Tsuruta, K. Hamada, H.T. Takeshita, H. Tanaka, T. Kiyobayashi, T. Takano, N. Kuriyama, *Int. J. Hydrogen Energy* 28 (2003) 1121.
- [3] R. Ströbel, M. Oszcipok, M. Fasil, B. Rohland, L. Jörissen, J. Garche, *J. Power Sources* 105 (2002) 208.
- [4] C. Lamy, J.-M. Léger, *J. Phys. IV* 4 (1994) C1.
- [5] J.S. Bett, H.R. Kunz, A.J. Aldykiewicz Jr., J.M. Fenton, W.S. Bailey, D.V. Mc Grath, *Electrochim. Acta* 43 (1998) 3645.
- [6] S. Wasmus, A. Küwer, *J. Electroanal. Chem.* 461 (1999) 14.
- [7] C. Coutanceau, A.F. Rakotondrainibe, A. Lima, E. Garnier, S. Pronier, J.-M. Léger, C. Lamy, *J. Appl. Electrochem.* 34 (2004) 61.
- [8] E.A. Batista, G.R.P. Malpass, A.J. Motheo, T. Iwasita, *J. Electroanal. Chem.* 571 (2004) 273.
- [9] F. Vigier, C. Coutanceau, F. Hahn, E.M. Belgsir, C. Lamy, *J. Electroanal. Chem.* 563 (2004) 81.
- [10] X.H. Xia, H.-D. Liess, T. Iwasita, *J. Electroanal. Chem.* 437 (1997) 233.
- [11] C. Lamy, S. Rousseau, E.M. Belgsir, C. Coutanceau, J.-M. Léger, *Electrochim. Acta* 49 (2004) 3901.
- [12] M.K. Ravikumar, A.K. Shukla, *J. Electrochem. Soc.* 143 (1996) 2601.
- [13] X. Ren, M.S. Wilson, S. Gottesfeld, *J. Electrochem. Soc.* 143 (1996) L12.
- [14] A.K. Shukla, C.L. Jackson, K. Scott, R.K. Raman, *Electrochim. Acta* 47 (2002) 3401.
- [15] F. Vigier, C. Coutanceau, A. Perrard, E.M. Belgsir, C. Lamy, *J. Appl. Electrochem.* 34 (2004) 439.
- [16] W.J. Zhou, W.Z. Li, S.Q. Song, Z.H. Zhou, L.H. Jiang, G.Q. Sun, Q. Xin, K. Pouliantitis, S. Kontou, P. Tsiakaras, *J. Power Sources* 131 (2004) 217.
- [17] H. Hitmi, E.M. Belgsir, J.-M. Léger, C. Lamy, O. Lezna, *Electrochim. Acta* 39 (1994) 407.
- [18] T. Iwasita, E. Pastor, *Electrochim. Acta* 39 (1994) 531.
- [19] J.-M. Léger, S. Rousseau, C. Coutanceau, F. Hahn, C. Lamy, *Electrochim. Acta* 50 (2005) 5118.
- [20] G.A. Camara, R.B. de Lima, T. Iwasita, *Electrochem. Commun.* 6 (2004) 812.
- [21] V. Pacheco Santos, G. Tremiliosi-Filho, *J. Electroanal. Chem.* 554–555 (2003) 395.
- [22] S. Rousseau, PhD thesis, University of Poitiers, France, 2004.
- [23] A. Lima, C. Coutanceau, J.-M. Léger, C. Lamy, *J. Appl. Electrochem.* 31 (2001) 379.
- [24] H. Bönemann, W. Brijoux, R. Brinkmann, E. Dinjus, T. Jousen, B. Korall, *Angew. Chem. Int. Engl.* 30 (1991) 1312.
- [25] L. Dubau, C. Coutanceau, E. Garnier, J.-M. Léger, C. Lamy, *J. Appl. Electrochem.* 33 (2003) 419.
- [26] L. Dubau, F. Hahn, C. Coutanceau, J.-M. Léger, C. Lamy, *J. Electroanal. Chem.* 554–555 (2003) 407.
- [27] W.J. Zhou, S.Q. Song, W.Z. Li, G.Q. Sun, Q. Xin, S. Kontou, K. Pouliantitis, P. Tsiakaras, *Solid State Ionics* 175 (2004) 797.
- [28] W.J. Zhou, S.Q. Song, W.Z. Li, Z.H. Zhou, G.Q. Sun, Q. Xin, S. Douvartzides, P. Tsiakaras, *J. Power Sources* 140 (2005) 50.
- [29] S. Song, G. Wang, W. Zhou, X. Zhao, G. Sun, Q. Xin, S. Kontou, P. Tsiakaras, *J. Power Sources* 140 (2005) 103.
- [30] S. Song, W. Zhou, Z. liang, Rui Cai, G. Sun, Q. Xin, V. Stergiopoulos, P. Tsiakaras, *Appl. Catal. B* 55 (2004) 65.
- [31] W. Watanabe, S. Motoo, *J. Electroanal. Chem.* 60 (1975) 267.
- [32] T. Iwasita, E. Pastor, *Electrochim. Acta* 39 (1994) 547.
- [33] R.A. Rightmire, R.L. Rowland, D.L. Boos, D.L. Beals, *J. Electrochem. Soc.* 111 (1964) 242.
- [34] P. Waszczuk, A. Wieckowski, P. Zelenay, S. Gottesfeld, C. Coutanceau, J.-M. Léger, C. Lamy, *J. Electroanal. Chem.* 511 (2001) 55.